Bartłomiej SZAFRANIAK, Paweł ZYDROŃ, and Łukasz FUŚNIK

AGH University of Science and Technology, Krakow, Poland

doi:10.15199/48.2020.01.11

Analysis of the influence of unequal current distribution on the heating of parallel connected LV MOV surge arresters

***Abstract**. In low-voltage (LV) electrical networks metal-oxide varistor (MOV) surge arresters connected in parallel are often used against overvoltages. The paper presents the results of laboratory experiments, during which pairs of parallel connected MOV surge arresters were subjected to surges of specified energy. The tests determined energy distribution between surge arresters for AC burst voltage stresses, temperatures recorded on their surface using contact sensors and temperature distribution images (IR thermograms). The analysis of results and conclusions are also presented.*

***Streszczenie.** W sieciach niskiego napięcia stosowane są zwykle tlenkowe ograniczniki przepięć. W artykule przedstawiono wyniki badań, podczas których pary równolegle połączonych ograniczników poddano działaniu narażeń o określonej energii. Badano rozkład energii pomiędzy ograniczniki dla narażeń przebiegami AC oraz rejestrowano termogramy IR i temperatury na ich powierzchni, mierzone czujnikami kontaktowym. Przedstawiono analizę wyników badań i wnioski. (**Analiza wpływu nierównomiernego rozpływu prądu na nagrzewanie się równolegle połączonych tlenkowych ograniczników przepięć niskiego napięcia**).*

Keywords: metal-oxide varistor, surge arrester, heating, parallel working, unequal current distribution.
Słowa kluczowe: warystor tlenkowy, ogranicznik przepięć, nagrzewanie, praca równoległa, nierównomierny rozpływ prądu.

Introduction

The contemporary requirements for high reliability of electrical devices and instruments make it necessary to protect all apparatus working in electrical networks against voltage surges that can arise in them. Overvoltages arising and propagating in networks can cause unacceptable level of voltage stresses destructively acting on electrical insulation systems. For protection of electrical devices and proper insulation coordination, various methods of mitigation and limitation of surges are applied, depending on characteristic of occurring overvoltages and specific properties of protected objects [1-7]. Currently, the most commonly used solution for this purpose is the use of surge arresters containing ZnO metal-oxide varistors (MOSA – Metal Oxide Surge Arrester) as voltage limiting devices. MOSAs are used at all voltage levels, from low voltage (LV), through medium voltage (MV) up to high (HV), extra- and ultra-high (EHV and UHV) voltages.

The physical mechanism of electric current conduction in the varistor is complex due to the influence of the varistor material properties and non-linear phenomena occurring at the boundaries of grains that build its polycrystalline structure [8-10]. The observed result is a non-linear dependence of the current flowing through the varistor from the voltage applied to its electrodes, which makes it very useful as a voltage stabilizing element. The strongly non-linear *current-voltage* (or *electric field* E - *current density* J, Fig. 1) characteristic of the MOV is described by the formula:

$$I = k \cdot V^{\alpha} \tag{1}$$

where: I – current flowing through the varistor; V – voltage on the varistor; k, α – constants, depending on the materials and parameters of the varistor production process.

In the pre-breakdown range of ZnO varistor *current-voltage* characteristic (Fig. 1), the resistive component of the varistor leakage current is many times smaller than the capacitive one. Experimentally observed static *current-voltage* characteristics in this region are almost linear (ohmic-type) but simultaneously very sensitive on the temperature of the varistor. Because of physical mechanism, resistive current increases significantly together with increase of varistor temperature.

In the voltage stabilization range of ZnO varistor *current-voltage* characteristic, clamping voltage shows a relatively small change in the wide range of varistor currents. For very large currents, in the saturation range, the increase of the voltage on the varistor is the result of the ZnO grain resistivity influence.

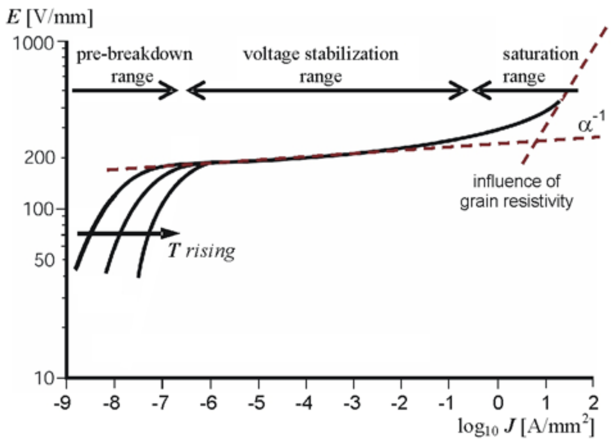

Fig.1. A typical $E = f(J)$ characteristic of zinc oxide varistor

Varistors are usually produced in the form of discs. Disc thickness determines the clamping voltage value and its circular area the highest value of the surge current, so the volume of a disk is related to the varistor energy absorption capacity. To improve the overvoltage protection of devices installed in electrical networks and increase the capacity to absorb energy of overvoltages MOSAs are used in parallel, and are placed in different points of an electric network (at terminals of protected devices) or multiplied at terminals of a single protected device. The last one solution in practice causes problems with equal overvoltage energy dissipation, related to the differences in *current-voltage* characteristics of parallel mounted varistors [11-15].

Paper presents the results and analyzes of experimental investigations carried-out on the two parallel connected low voltage MOSAs of the same type, subjected to the sequence of AC voltage bursts stressing structures of their varistors. The results of voltage and currents measurements and evaluated energies absorbed by each MOSA as well as the temperature changes recorded by two methods on the surfaces of the arresters enclosure are presented and discussed.

Tested objects, experimental setup and procedure

A. Tested objects

For the laboratory experiments were used commercially available low voltage MOV surge arresters (Fig. 2) with the basic technical parameters presented in Table 1.

Fig. 2. Tested low voltage surge arresters with a polymer housing

Table 1. Selected parameters of tested MOSA

Parameter	Value
Continuous operating voltage U_c [V]	280
Nominal surge current (for 8 μs /20 μs pulse) I_n [kA]	10
Clamping voltage U_{pn} at I_n [V]	1010
Maximum surge current (for 8μs /20μs pulse) I_{max} [kA]	40
Max. voltage protection level U_{pmax} at I_{max} [V]	1440
Energy absorption capability [kJ/V]	5/1000

B. Experimental setup

Used during laboratory experiments system for testing of parallel connected low-voltage MOSAs (Fig. 3, 4, 5) allowed generation of voltage waveforms of AC burst in programmed time sequences. During the tests, the digital storage oscilloscope (Tektronix TDS 784D) recorded the following waveforms: voltage at surge arresters (Ch1) and currents of each of two arresters (Ch2 / Ch3); indirectly by measuring of voltages on two precision 4-terminal 0.1 Ω resistors.

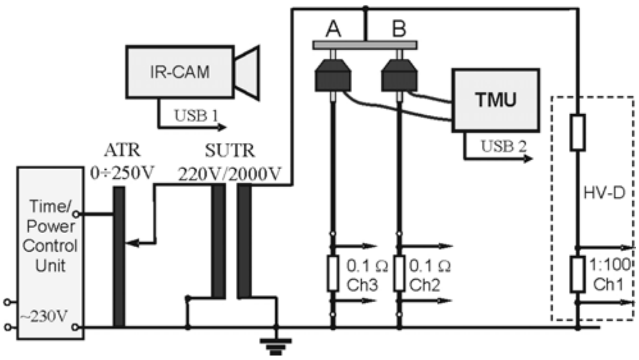

Fig. 3. General scheme of laboratory system for testing of parallel-connected low-voltage MOSAs (ATR – autotransformer; SUTR – step-up transformer; IR-CAM – infrared camera; TMU – 2-channel temperature measurement unit; HV-D – high voltage divider).

The processes of heating and cooling of surge arresters subjected to voltage stresses of the AC burst sequence were observed by infrared camera to take thermograms of the MOSAs housing surfaces and by a contact temperature measurement system containing two K-type thermocouples. Both temperature measuring instruments were read using the USB serial interface (USB 1 / USB 2).

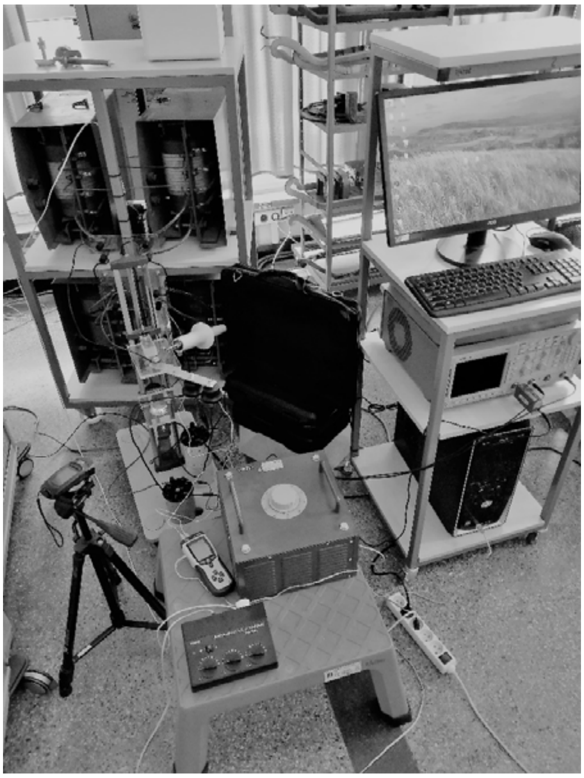

Fig. 4. Measuring stand for parallel-connected LV MOSAs tests - general view

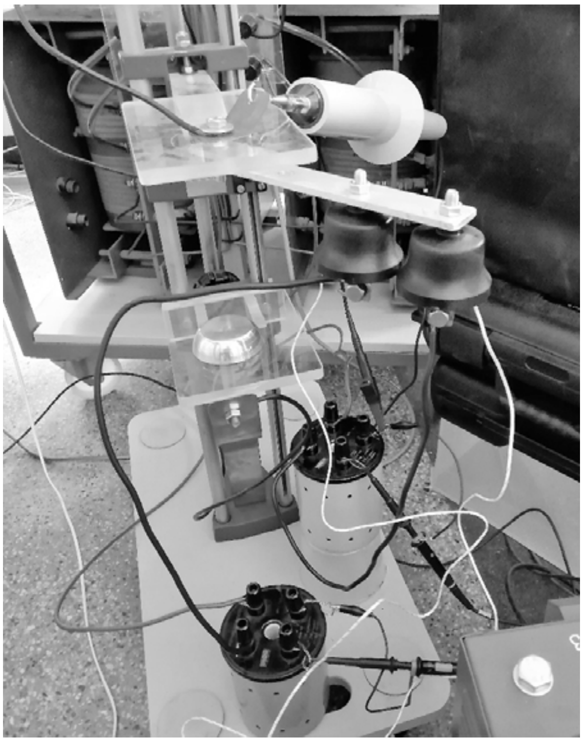

Fig. 5. Tested LV MOSAs with a high voltage probe and two series-connected 4-terminal resistors used for measuring individual currents of parallel varistors

C. Laboratory experiment procedure

In the first stage of the test procedure, from the group of about twenty of the same type low voltage MOSAs, two arresters (signed as A and B MOSA) with noticeably different clamping voltage values were selected. Then, for their parallel connection, a programmed 50 Hz AC burst voltage sequence was realized. Each single AC voltage burst fed to the parallel connected surge arresters had a width of about 1.2 second. The entire energy pulses sequence contained five successive AC bursts, separated by a time interval of about 3 minutes. The first two were bursts with lower voltage and therefore also lower energy (respectively 100 J and 94 J). The next three were bursts with a slightly higher voltage, but with significantly higher energy (respectively 1326 J, 1360 J, and 1366 J).

Results of experiment

Figures 6 and 7 present digitally recorded waveforms of voltage and currents of surge arresters, acquired for low and high energy 50 Hz AC bursts during the test sequence. Table 2 summarizes the energy values absorbed individually by MOSAs A and B in the AC bursts sequence.

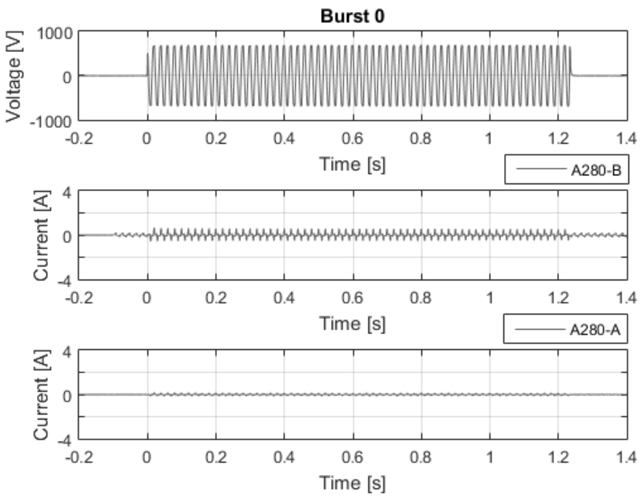

Fig. 6. Recorded AC burst waveforms for low-energy stimulation: voltage (top), current of MOSA B (middle), and current of MOSA A (bottom)

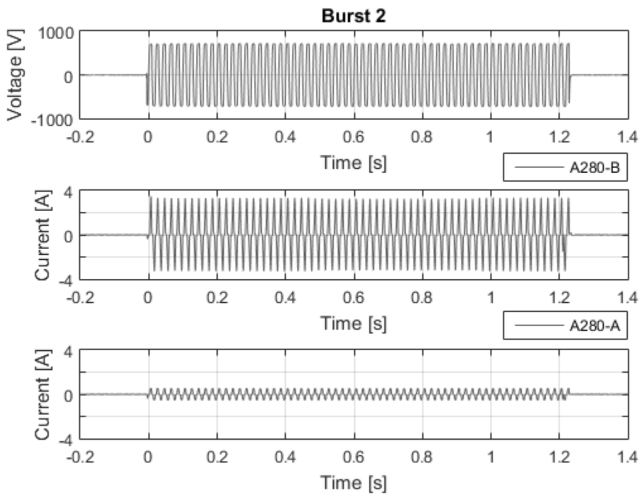

Fig. 7. Recorded AC burst waveforms for high-energy stimulation: voltage (top), current of MOSA B (middle), and current of MOSA A (bottom).

Table 2. Energy of AC bursts registered for MOSAs A and B

Time	t_0	t_1	t_2	t_3	t_4
E_A [J]	24	23	220	267	268
E_B [J]	76	71	1106	1093	1098

Figure 8 presents plots of the temperatures on the surface of MOSAs A and B, recorded using a measuring system with two K-type thermocouples. A significant temperature difference between these two surge arresters is visible, resulting from significantly different energy dissipated in them. The same effects can be seen when analyzing the results of infrared observation of the housing of the two tested MOSAs. Figure 9 shows the thermal state images of MOSAs A and B surfaces in the time moments corresponding to the points marked on the temperature plots in Figure 8.

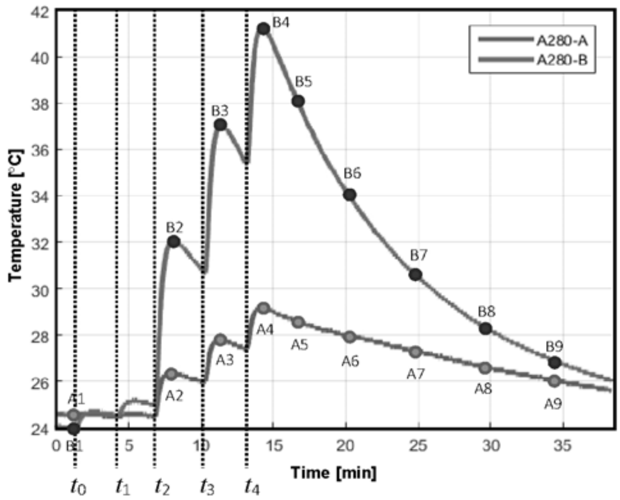

Fig. 8. Plots of the temperatures on the bottom surface of MOSAs A and B, recorded using a measuring system with two K-type thermocouples

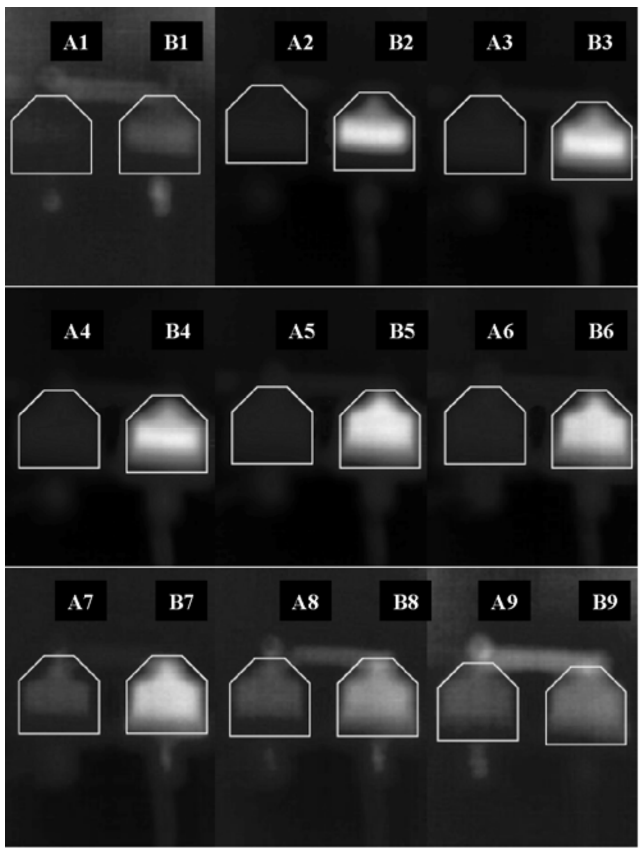

Fig. 9. MOSA A and B thermograms recorded by the infrared camera in the moments of time indicated in the temperature plots shown in Figure 8. (Note: temperature scales are not identical on all thermograms)

Discussion of results and conclusions

In the analyzed case, the energy distribution between A and B MOSAs ranged from approximately 1:3 for low energy AC bursts to approximately 1:4 for high energy ones. This indicates very unfavorable working conditions of the B arrester, dissipating the main part of the AC bursts energy.

The use of parallel connected MOSAs causes problems related to uneven distribution of surge currents between used protecting devices. This results in an uneven energy and thermal load of the varistors of individual arresters. The performed test confirms this problem for low voltage MOSAs of the same type, without the selection which allows proper cooperation of surge arresters with similar *current-voltage* characteristics.

The strongly non-linear character of equation (1) causes that small differences in the parameters of two neighboring characteristics result in large difference of currents for the same voltage on parallel connected varistors (Fig. 10).

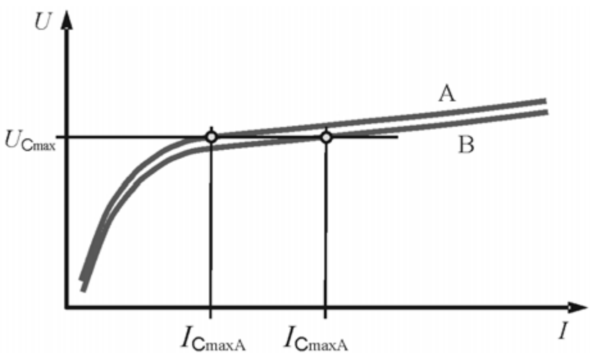

Fig. 10. Influence of differences in *current-voltage* characteristics on MOSA A and B currents (U_{Cmax} – maximum value of clamping voltage; I_{CmaxA} – MOSA A current at U_{Cmax}; I_{CmaxA} – MOSA B current at U_{Cmax})

The long time constant of the low voltage MOSA cooling process [17] causes that repeated energy stimulus successively accumulates its effect, raising the temperature of the varistors. Then, the uneven distribution of the dissipated energy accelerates thermal aging of the varistor of the more loaded surge arrester. To limit this phenomenon, you can:

1) make a selection of surge arresters connected in parallel in terms of high similarity of the *current-voltage* characteristics;
2) use additional low value resistors connected in series with varistors, affecting the *resultant current-voltage* characteristics [11].

Unfortunately, the second solution affects the overvoltage mitigation at protected devices in the same time.

Acknowledgement

The presented researches were financed by the Polish Ministry of Science and Higher Education, by subvention for Faculty of Electrical Engineering, Automatics, Computer Science and Biomedical Engineering of AGH University of Science and Technology, Krakow, Poland.

***Authors**: mgr inż. Bartłomiej Szafraniak, dr hab. inż. Paweł Zydroń, mgr inż. Łukasz Fuśnik, AGH University of Science and Technology, Dept. of Electrical and Power Engineering, al. Mickiewicza 30, 30-059 Kraków, Poland, E-mail: szafrani@agh.edu.pl, pzydron@agh.edu.pl, lfusnik@agh.edu.pl.*

REFERENCES

[1] Hasse P., Overvoltage protection of low-voltage systems, 2nd ed., ISBN 978-0852967812, IET, 2000.
[2] Paul D., Low-voltage power system surge overvoltage protection, *IEEE Trans. Ind. Appl*., 37 (2001), No. 1, 223–229
[3] Paolone M., Nuci C. A., Petrache E., Rachidi F., Mitigation of lightning-induced overvoltages in medium voltage distribution lines by means of periodical grounding of shielding wires and of surge arresters: modeling and experimental validation, *IEEE Trans. Power Del*., 19 (2004), No. 1, 423–431
[4] Jaroszewski M., Pospieszna J., Ranachowski P., Rajmund F., Modeling of overhead transmission lines with line surge arresters for lightning, International CIGRÉ Colloq., Cavtat, Croatia, May 2008
[5] Kuczek T, Stosur M., Szewczyk M., Piaseczki W., Steiger M., Investigation on new mitigation method for lightning overvoltages in high-voltage power substations, *IET Gen., Transm. Distrib*., 7 (2013), No. 10, 1055–1062
[6] Florkowski M., Furgał J., Kuniewski M., Propagation of overvoltages in distribution transformers with silicon steel and amorphous cores, *IET Gener. Transm. Distrib*., 9 (2015), No. 16, 2736–2742
[7] Szewczyk M, Kuniewski M, Controlled voltage breakdown in disconnector contact system for VFTO mitigation in gas-insulated switchgear (GIS), *IEEE Trans. Power Del*., 32 (2017), No. 5, 2360–2366
[8] Matsuoka M., Nonohmic properties of zinc oxide ceramics, *Jpn. J. Appl. Phys*., 10 (1971), No. 6, 736–746
[9] Eda K., Zinc oxide varistors, *IEEE Electr. Insul Mag*., 5 (1989), No. 6, 28–41
[10] Maran G. D., Levinson L. M., Philipp H. R., Theory of conduction in ZnO varistors, *J. Appl. Phys*., 50 (1979), 2799–2812
[11] Putrus G. A., Ran L., Ahmed M. M. R., Improving current sharing between parallel varistors, ISIE 2001 - IEEE Int. Symp. Industrial Electronics, Pusan, Korea, June 2001
[12] J. He, et. al, Electrical parameter statistic analysis and parallel coordination of ZnO varistors in low-voltage protection devices, *IEEE Trans. Power Del*., 10 (2005), No. 1, 131-137
[13] Tuczek M. N., Broker M., Hinrichsen V., Galer R., Effects of continuous operating voltage stress and AC energy injection on current sharing among parallel-connected metal–oxide resistor columns in arrester banks, *IEEE Trans. Power Del*. 30 (2015), No. 3, 1331-1337
[14] Tsujimoto Y., Tsukamoto N., Tsuge R., Baba Y., Surge withstand capability of parallel-connected metal oxide varistors, 34th Int. Conf. Lightning Protection ICLP 2018, Rzeszow, Poland, Sept. 2018
[15] Cuixia Z., UHV transmission technology, Elsevier Science Publishing Co Inc., ISBN: 978-0128051931, 2017
[16] Ahmed M.M.R., Putrus G.A., Ran L., Penlington R., Measuring the energy handling capability of metal oxide varistors, CIRED 2001 16th Int. Conf. and Exhib. on Electr. Distrib., Part 1: Contributions, IEE Conf. Publ. no. 482, Amsterdam, The Netherlands, June 2001
[17] Szafraniak B., Bonk M., Fuśnik L., Zydron P., Influence of high current impulses and 50 Hz AC bursts on the temperature of low-voltage metal-oxide surge arresters, 2018 Progress in Applied Electr. Engineering (PAEE), Koscielisko (Zakopane), Poland, June 2018